Journal of Biomolecular NMR, 9 (1997) 323–328
ESCOM

J-Bio NMR 439

χ_1 angle information from a simple two-dimensional NMR experiment that identifies trans $^3J_{NC'\gamma}$ couplings in isotopically enriched proteins

Jin-Shan Hu and Ad Bax

Laboratory of Chemical Physics, National Institutes of Diabetes and Digestive and Kidney Diseases, National Institutes of Health, Bethesda, MD 20892-0520, U.S.A.

Received 24 January 1997
Accepted 26 February 1997

Keywords: χ_1 angle; Calmodulin; Carbon-nitrogen J coupling; Quantitative J correlation; Stereospecific assignment; Ubiquitin

Summary

New quantitative J correlation experiments are used for measuring all two- and three-bond couplings between ^{15}N and aliphatic side-chain carbons in proteins uniformly enriched in ^{13}C and ^{15}N. Results show that $^3J_{NC\beta}$ and $^2J_{NC\beta}$ invariably are very small. Therefore, a simple and relatively sensitive two-dimensional spin-echo difference experiment can be used to identify residues with a $^3J_{NC\gamma}$ coupling substantially larger than 1 Hz, indicative of a trans arrangement between N and C^γ. This measurement therefore provides χ_1 angle information for residues with an aliphatic C^γ carbon, and thereby also aids in making stereospecific assignments of H^β resonances. Experiments are demonstrated for ubiquitin and for a complex between calmodulin and a 26-residue peptide.

Information regarding the rotameric state of χ_1 side-chain torsion angles in proteins can be obtained from $^3J_{H\alpha H\beta}$ couplings and intraresidue and sequential NOEs (Wagner et al., 1987; Güntert et al., 1989; Kraulis et al., 1989; Clore et al., 1991). However, as a result of extensive spectral overlap, quantitative measurement of these parameters is not always straightforward. Recently, we have shown that for aromatic residues χ_1 can be determined from two simple heteronuclear spin-echo difference experiments (Hu et al., 1997). Because the aromatic $^{13}C^\gamma$ resonances are the only ones resonating in the 110–140 ppm region within three bonds from the backbone ^{15}N and $^{13}C'$ atoms, measurement of $^3J_{NC\gamma}$ and $^3J_{C'C\gamma}$ from such 2D difference spectra is very straightforward.

Measurement of $^3J_{C'C\gamma}$ in aliphatic residues is also readily possible, and is obtained as a 'by-product' when measuring the interresidue $^3J_{C'C\beta}$ coupling (Hu and Bax, 1997). Here, we focus on the complementary coupling, $^3J_{NC\gamma}$. We will show that the intraresidue $^2J_{NC\beta}$ is always smaller than 0.9 Hz, and, in contrast to $^3J_{C'C\beta}$, $^3J_{NC\beta}$ is invariably very small ($\leq \sim 0.3$ Hz) for all values of the intervening torsion angle (ψ). The same has been reported for $^3J_{NH\alpha}$, which also depends on ψ and ranges from –2 to 0 Hz (Wang and Bax, 1995). Therefore, $^{13}C^\gamma$ nuclei are the only carbons resonating in the 40–10 ppm region which can have J couplings to the backbone ^{15}N larger than 1 Hz. As demonstrated in this paper, this permits measurement of the $^3J_{NC\gamma}$ coupling by means of a relatively sensitive 2D difference experiment.

Previous measurement of $^3J_{NC}$ was largely restricted to couplings involving methyl groups which, as a result of their favorable relaxation properties and threefold degenerate proton resonance, offer exceptional resolution and sensitivity (Vuister et al., 1993). The new methods are equally applicable to all residues with aliphatic C^γ carbons, and results are shown to be in excellent agreement with these earlier measurements.

In order to show that $^3J_{NC\beta}$ and $^2J_{NC\beta}$ are very small, we first describe the 3D experiment (Fig. 1) used for their measurement. Then we describe the ^1H-^{15}N-$\{^{13}C^\gamma\}$ difference experiment (Fig. 2), which offers a simpler and more sensitive way for measuring $^3J_{NC\gamma}$.

The pulse scheme shown in Fig. 1 is of the quantitative J correlation type, aimed at the measurement of $J_{NC\gamma}$, and the scheme is referred to as HNCG. The experiment is analogous to earlier experiments for measurement of ^{15}N-

Supplementary Material available: One table containing $^3J_{NC\gamma}$ couplings recorded with the 2D spin-echo difference method for a complex between calmodulin and a 26-residue fragment of skeletal muscle myosin light chain kinase.

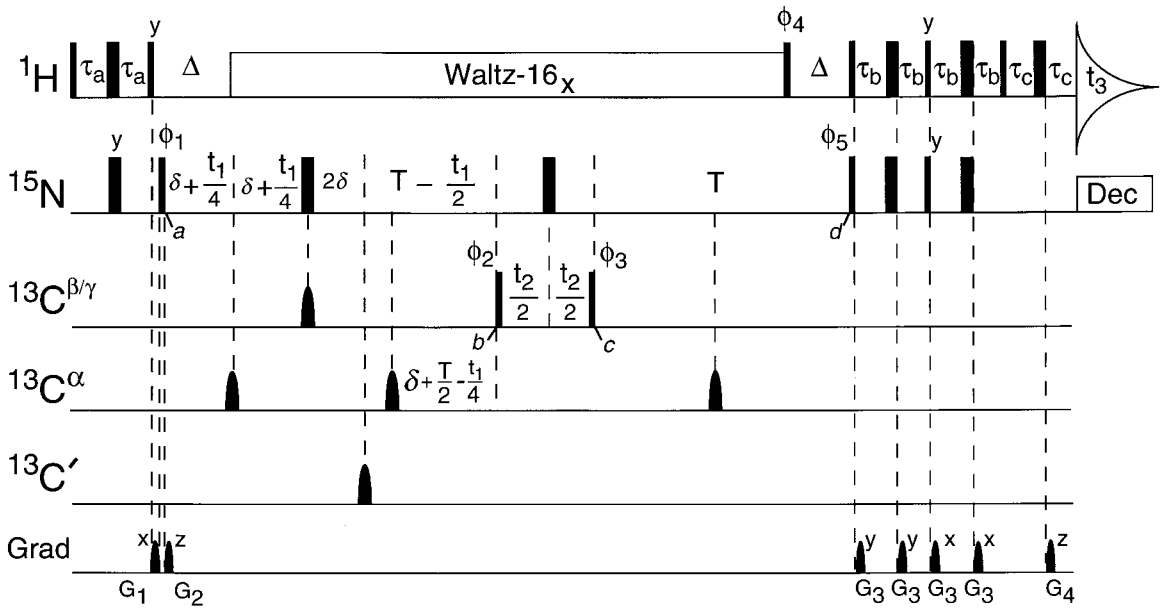

Fig. 1. Pulse sequence of the 3D HNCG experiment. Narrow and wide pulses denote 90° and 180° flip angles, respectively, and unless indicated the rf phase is x. ^{1}H decoupling is applied using a WALTZ-16 modulation scheme ($\gamma_H B_1 = 3.3$ kHz), with the carrier at the H_2O resonance and the rf phase ±x. The $^{13}C^{\beta/\gamma}$ (24 ppm) shaped pulse (4.4 ms) has a hyperbolic secant envelope with a squareness level, μ, of 6 (Silver et al., 1984), and an inversion bandwidth (>95%) of ±2 kHz. $^{13}C^{\alpha}$ pulses (58 ppm) are G_3-shaped (Emsley and Bodenhausen, 1990) and have durations of 1.25 ms (for 151 MHz ^{13}C). The ^{13}C′ 180° pulse is sine-bell shaped and has a duration of 300 μs. The $90°_{\phi 2}$ and $90°_{\phi 3}$ $^{13}C^{\beta/\gamma}$ pulses are rectangular and have durations of 42 μs, with a null in the excitation profile at the ^{13}C′ frequency. Delay durations: $\delta = 2.65$ ms; $\Delta = 5.3$ ms; $T \approx 100$ ms (see text); $\tau_a = 2.25$ ms; $\tau_b = 2.65$ ms; $\tau_c = 0.46$ ms. Phase cycling: $\phi_1 = 2(x),2(-x)$; $\phi_2 = x,-x$; $\phi_3 = 2(x),2(-x)$; $\phi_4 = 2(y),4(-y),2(y)$; $\phi_5 = -x$; receiver = x,–x. Phase cycling of ϕ_4 suppresses t_1-noise-like artifacts resulting from NH_2 groups (Bax et al., 1990). For the 2D reference spectrum, t_2 is set at its minimum value, and receiver = 2(x),2(–x). Quadrature detection in the t_1 dimension is obtained by inverting the polarity of G_2 together with ϕ_5, with data stored separately, in order to obtain Rance–Kay-style data (Kay et al., 1992). Quadrature detection in the t_2 dimension is obtained in the regular States-TPPI manner, by incrementing ϕ_2. Gradients (sine-bell shaped; 25 G/cm at center): $G_{1,2,3,4} = 3.75$, 1.5, 0.5, and 0.1564 ms. The directions of the gradients are marked in the figure. Gradient G_2 may be applied either during the first or during the second Δ period. In either case, signal attenuation resulting from protein translational diffusion between gradients G_2 and G_4 is negligible for the weak gradients used.

$^1H^{\beta}$ J couplings (HNHB; Archer et al., 1991), ^{13}C′-H^{β} J couplings (HN(CO)HB; Grzesiek et al., 1992), and ^{13}C′-$^{13}C^{\beta/\gamma}$ J couplings (HN(CO)C; J.-S. Hu and A. Bax, manuscript submitted). The description of the experiment is therefore very similar and only a condensed version will be presented here. $^1H^N$ magnetization is transferred to ^{15}N (time point a in Fig. 1). In order to minimize the decay of ^{15}N transverse magnetization during the rather long $2T + 4\delta$ period, ^{15}N magnetization is decoupled from ^{1}H by means of continuous ^{1}H decoupling, instead of by 180° ^{1}H pulses (Bax et al., 1990; Grzesiek and Bax, 1992; Peng and Wagner, 1992). ^{15}N evolution is of the constant-time variety (Bax et al., 1979; Sørensen, 1990), and ^{15}N-$^{13}C^{\beta/\gamma}$ dephasing is active during the period between time points a and b for a total duration $T + 4\delta$, because a $^{13}C^{\beta/\gamma}$ 180° pulse is applied simultaneously with the 180° ^{15}N pulse. Dephasing resulting from $^1J_{NC}\alpha$ and $^2J_{NC}\alpha$ is refocused by means of two selective $^{13}C^{\alpha}$ pulses, applied at the midpoint between the $90°_{\phi 1}$ ^{15}N pulse and the following 180° ^{15}N pulse, and midway between this 180° pulse and $90°_{\phi 2}$ ($^{13}C^{\beta/\gamma}$). Dephasing resulting from $^1J_{C'N}$ is refocused just prior to transfer of the magnetization back to H^N (time-point d) by the selective 180° ^{13}C′ pulse, and $^1J_{C'N}$ may therefore be ignored.

Assuming that the ^{15}N chemical shift is on-resonance, the density matrix, σ_b, at time point b is described by

$$\begin{aligned}\sigma_b = {} & N_x \Pi_p \cos[\pi J_{Np}(T + 4\delta)] \\ & + \textstyle\sum_p 2N_y C_z^p \sin[\pi J_{Np}(T + 4\delta)] \\ & \Pi_{q \neq p} \cos[\pi J_{Nq}(T + 4\delta)] + \ldots\end{aligned} \quad (1)$$

where N_x and N_y are the ^{15}N spin operators, the product and summation extend over all aliphatic side-chain carbons, and '...' refers to terms with multiple ^{13}C operators. Terms with two ^{13}C operators are eliminated by the phase cycle, and higher order terms are vanishingly small. The $90°_{\phi 2}$ ^{13}C pulse transforms the $2N_yC_z^p$ term of Eq. 1 into two-spin coherence, $-2N_yC_y^p$. ^{15}N chemical shift evolution during the t_2 period is eliminated by the 180° pulse, applied at the midpoint of t_2, and at time c the $90°_{\phi 3}$ ^{13}C pulse transforms the $-2N_yC_y^p\cos(\omega_p t_2)$ back into $-2N_yC_z^p\cos(\omega_p t_2)$, where ω_p is the chemical shift of C^p. Subsequently, ^{15}N magnetization rephases for a duration T, and at time d, the $\cos(\omega_p t_2)$-modulated signal, which gives rise to the cross peak with C^p, has an amplitude, I_C, given by:

$$\begin{aligned}I_C = {} & A \sin[\pi J_{Np}(T + 4\delta)] \sin(\pi J_{Np} T) \\ & \Pi_{q \neq p} \cos[\pi J_{Nq}(T + 4\delta)] \cos(\pi J_{Nq} T)\end{aligned} \quad (2)$$

where A is a constant that depends on ^{1}H and ^{15}N relaxation times and on numerous instrumental factors. Because of the requirements $2\delta \geq \Delta = 1/(2^1J_{NH})$ (in order to avoid ^{15}N evolution during Δ, in the absence of ^{1}H decoupling), the J_{NC}-dephasing period is 4δ longer than the rephasing period. Using $\sin(\alpha+2\beta)\sin(\alpha) \approx \sin^2(\alpha+\beta)$ for $\beta \ll \pi/2$, Eq. 2 may be rewritten as:

$$I_C = A \sin^2[\pi J_{Np}(T+2\delta)]\, \Pi_{q\neq p} \cos^2[\pi J_{Nq}(T+2\delta)] \quad (3)$$

Magnetization at time d which has not evolved as ^{15}N-^{13}C multiple-quantum coherence between time points b and c, and which can be selected by the alternate receiver phase cycle indicated in the legend to Fig. 1, can be used as a reference signal, of intensity I_R, given by:

$$I_R = -A\, \Pi_q \cos^2(\pi J_{Nq} T + 2\delta) \quad (4)$$

^{15}N magnetization is transformed back into ^{1}H coherence using the standard Rance–Kay gradient-enhanced transfer method (Palmer et al., 1991; Kay et al., 1992). The reference spectrum is detected in the ^{15}N-^{1}H 2D mode, whereas the correlation to ^{13}C is most conveniently carried out in a ^{15}N-^{13}C-^{1}H 3D fashion. Therefore, one way of calculating J_{Np} directly from the ratio of Eqs. 3 and 4 bypasses Fourier transformation in this t_2 dimension, i.e., the (t_1,t_3)-transformed signal, S(F1, $t_2 = 0$, F3), is compared with the 2D reference spectrum, S(F1, $t_2 = 0$, F3). The intensity of signal component p in S(F1, $t_2 = 0$, F3) is a factor $N_2F(\omega_2)$ smaller than its intensity after Fourier transformation in the t_2 dimension, where N_2 is the number of complex t_2 data points, and $F(\omega_2)$ is the average amplitude of the time domain signal component, relative to its first point, including the effect of apodization. Knowing the approximate T_2 value of C^p, and the number of ^{13}C nuclei directly coupled to it, $F(\omega_2)$ can be estimated to within ~5% (Hu and Bax, 1997). This then permits J_{Np} to be calculated from the ratio of the intensity in the 3D spectrum and the corresponding peak in the 2D reference spectrum.

As will be shown, the intraresidue $^2J_{NC\beta}$ coupling is invariably smaller than 0.9 Hz. The interresidue $^3J_{NC\beta}$ coupling, which is expected to show a Karplus-type dependence on the backbone angle ψ, is found to be even smaller. Therefore, besides $^{13}C^{\alpha}$, only the intraresidue $^{13}C^{\gamma}$ carbon can have a significant coupling to ^{15}N. $^3J_{NC\gamma}$ depends on the torsion angle χ_1, and trans values of ~2.1 Hz have previously been reported for Val and Ile residues,

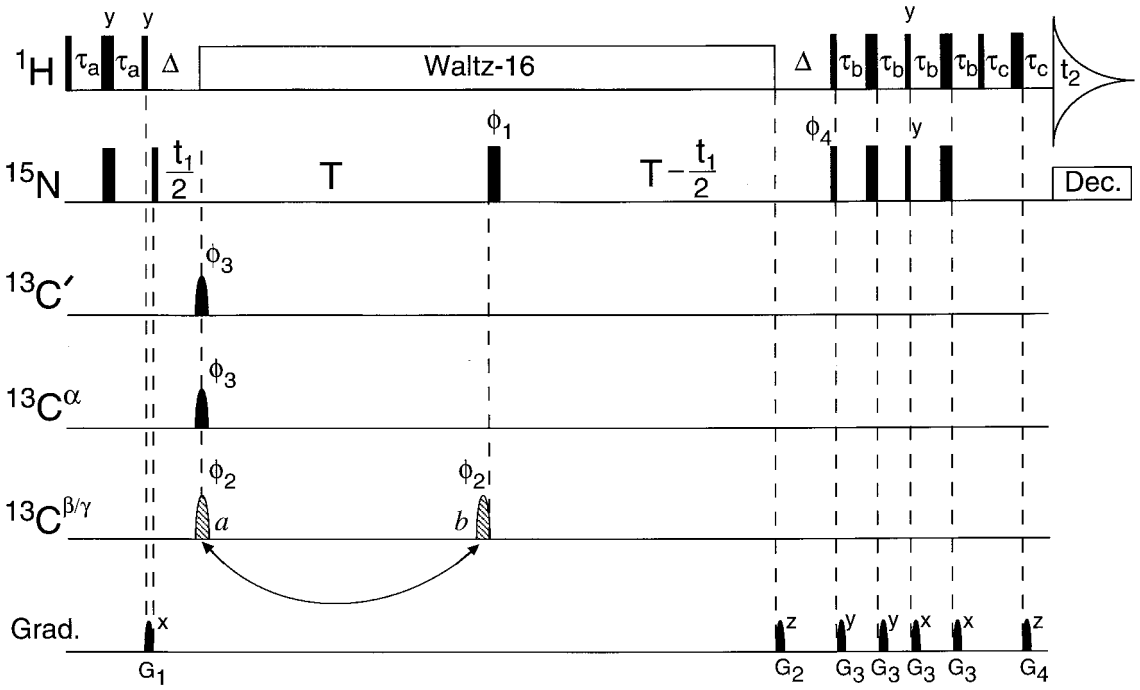

Fig. 2. Pulse sequence of the 2D $^1H^N$-^{15}N-{$^{13}C^{\gamma}$} difference experiment. The experiment is carried out twice, once with the $^{13}C^{\beta/\gamma}$ pulse in position a (reference), and once in position b (attenuated spectrum). Narrow and wide pulses denote 90° and 180° flip angles, respectively, and unless indicated the rf phase is x. ^{1}H decoupling is applied using a WALTZ-16 modulation scheme ($\gamma_H B_1 = 3.3$ kHz), with the carrier at the H_2O resonance. All shaped ^{13}C inversion pulses are of the hyperbolic secant type and have squareness levels, μ, of 6 for $^{13}C^{\alpha}/^{13}C^{\beta/\gamma}$, and $\mu = 3$ for ^{13}C' (Silver et al., 1984), and durations of 3 ms ($^{13}C^{\alpha}$), 4.4 ms ($^{13}C^{\beta/\gamma}$) and 1 ms (^{13}C'), for 151 MHz ^{13}C frequency. Delay durations: $\tau_a = 2.25$ ms; $\tau_b = 2.65$ ms; $\tau_c = 0.46$ ms; $\Delta = 5.3$ ms; $T \approx 100$ ms (see text). Phase cycling: ϕ_1 = x,y,–x,–y; ϕ_2 = 4(x),4(–x); ϕ_3 = 8(x),8(–x); ϕ_4 = –x; receiver = x,–x. Gradients (sine-bell shaped; 25 G/cm at center): $G_{1,2,3,4} = 2.5$, 2.0, 1.0, and 0.2074 ms. The directions of the gradients are marked in the figure. Quadrature detection in the t_1 dimension is obtained by inverting the polarity of G_2 together with ϕ_4, with data stored separately (Kay et al., 1992). Data with the $^{13}C^{\beta/\gamma}$ pulse in positions a and b are recorded in an interleaved manner and stored separately. The ^{13}C hyperbolic secant pulses were applied sequentially (first ^{13}C', then $^{13}C^{\alpha}$, then $^{13}C^{\beta/\gamma}$).

TABLE 1
$^3J_{NC\gamma}$, $^2J_{NC\beta}$ AND $^3J_{NC\beta}$ COUPLING CONSTANTS (Hz) IN HUMAN UBIQUITIN[a]

Residue	3D HNCG				2D ^{1}H-^{15}N-{C$^\gamma$}	
	$^3J_{NC\gamma 1}$	$^3J_{NC\gamma 2}$	$^2J_{NC\beta}$	$^3J_{NC\beta}$ [b]	$^3J_{NC\gamma}$ [c]	$^3J_{NC\gamma}$ [d]
Q2	0.92	–	0.69	0.30	1.16	0.95
I3	0.43	0.40	0.41[e]	< 0.3[e]	0.68	0[f]
V5	1.70	0.41	0.46	< 0.3	1.78	1.68[f]
K6	1.10	–	0.68	0.31	1.31	1.15
T7	–	0.88	[e]	[e]	0.98	[g]
L8	0.63	–	0.48[e]	[e]	0.71	0.11
T9	–	0.66	[e]	[e]	0.69	[g]
K11	1.40	–	0.73	< 0.3	1.60	1.48
T12	–	1.43	[e]	[e]	1.47	[g]
I13	0.53	1.33	0.41[e]	0.30[e]	1.46	1.32[f]
T14	–	1.29	[e]	[e]	1.34	[g]
L15	0.30	–	[e]	[e]	0.37	[g]
E16	1.15	–	0.73	0.29	1.50	1.36
V17	0.32	0.57	0.25	< 0.3	0.78	0.35[f]
E18	< 0.3	–	0.61	< 0.3	0.78	0.37
T22	–	0.66	[e]	[e]	0.71	[g]
I23	< 0.3	1.96	0.87	< 0.3	2.09	2.03[f]
V26	1.84	0.44	0.70	< 0.3	2.07	2.01[f]
K27	0.29	–	0.56	< 0.3	0.71	0.14
K29	0.40	–	0.59	< 0.3	0.74	0.24
I30	0.31	1.88	0.73	< 0.3	2.06	2.00[f]
K33	0.71	–	0.54	< 0.3	0.94	0.65
E34	0.42	–	0.31	< 0.3	0.58	0
I36	0.56	1.76	[e]	[e]	1.89	1.81[f]
Q40	0.39	–	0.56	< 0.3	0.70	0.09
Q41	< 0.3	–	0.41	< 0.3	0.55	0
R42	0.83	–	0.45	0.37	1.00	0.73
L43	0.35	–	[e]	[e]	0.58	[g]
I44	0.29	1.45	[e]	[e]	1.54	1.41[f]
K48	0.65	–	0.41	< 0.3	0.90	0.59
Q49	1.38	–	0.88	< 0.3	1.70	1.60
L50	0.37	–	0.34[e]	[e]	0.50	0
E51	0.47	–	0.44	< 0.3	0.66	0
R54	0.40	–	0.64	< 0.3	0.83	0.45
T55	–	0.73	[e]	[e]	0.80	[g]
L56	< 0.3	–	0.54[e]	[e]	0.39	0
I61	0.36	1.95	0.74	0.36	2.11	2.06[f]
Q62	0.34	–	0.35	< 0.3	0.67	0
K63	0.82	–	0.58	< 0.3	1.06	0.81
E64	0.33	–	0.27	< 0.3	0.61	0
T66	–	1.58	[e]	[e]	1.58	[g]
L67	0.38	–	0.33[e]	[e]	0.33	[g]
L69	1.75	–	0.38[e]	[e]	1.87	1.79
V70	1.12	–	0.47	0.22	1.31	1.14[f]
L71	0.65	–	0.35[e]	0.21[e]	0.69	0
L73	< 0.3	–	0.35[e]	[e]	0.69	0
R74	0.94	–	0.51	< 0.3	1.09	0.86

[a] Couplings are reported for all residues with a $^{13}C^\gamma$ in the 38–10 ppm chemical shift range, except for Q31 and R72 (^{15}N-^{1}H overlap) and E24 (weak as a result of slow conformational exchange). Values have not been corrected for the finite ^{13}C T_1 values and underestimate the true values by ~10%.

[b] $^3J_{NC\beta}$ couplings between C^β of residue i and N of residue i + 1.

[c] Calculated from a ^{15}N-^{1}H-{$^{13}C^\gamma$} difference spectrum, using Eq. 5 and assuming $^2J_{NC\beta} = 0$ Hz.

[d] Calculated from Eq. 5 and assuming $^2J_{NC\beta} = 0.7$ Hz.

[e] No accurate values for $^2J_{NC\beta}$ and $^3J_{NC\beta}$ could be determined because $^{13}C^\beta$ resonates downfield of 38 ppm.

[f] Value reported corresponds to $\sim(^3J^2_{NC\gamma 1} + {}^3J^2_{NC\gamma 2})^{1/2}$.

[g] $^{13}C^\beta$ not inverted by $^{13}C^{\beta/\gamma}$ 180° pulse ($^{13}C^\beta$ downfield of 43 ppm).

whereas gauche values were found to be ~0.5 Hz. Therefore, an answer to the question whether $^3J_{NC\gamma}$ is large (≥1.7 Hz) or small (≤1 Hz) can be obtained from a simple and relatively sensitive 2D spin-echo difference experiment, as described below.

The pulse sequence for the ^{15}N-{$^{13}C^\gamma$} 2D spin-echo difference experiment is shown in Fig. 2. The description is analogous to that of the ^{13}C-{^{15}N} difference experiment (Vuister et al., 1993), which for sensitivity reasons was only applicable to cases where the ^{13}C is a methyl carbon. The experiment is carried out twice, once with the position of the $^{13}C^{\beta/\gamma}$ pulse at time point a, and once at time point b. In both schemes, ^{15}N dephasing resulting from $J_{C'N}$ and $J_{NC\alpha}$ is refocused at the end of the 2T period, immediately prior to the Rance–Kay-style transfer of magnetization back to H^N for observation. With the $^{13}C^{\beta/\gamma}$ pulse in position a, effects of $J_{NC\beta}$ and $J_{NC\gamma}$ are also refocused. However, with this pulse in position b, the net amount of ^{15}N transverse magnetization, antiphase only with respect to its attached proton H^N, is attenuated by a factor, K, given by:

$$K = \cos(2\pi\, {}^3J_{NC\gamma}T)\, \cos(2\pi\, {}^3J_{NC\gamma'}T)\, \cos(2\pi\, {}^3J_{NC\beta}T)\, \cos(2\pi\, {}^2J_{NC\beta}T) \quad (5)$$

where the $\cos(2\pi\, {}^3J_{NC\gamma'}T)$ term is only present for Ile and Val residues. The factor K is readily measured from the ratio of the attenuated spectrum and the reference spectrum. In calculating $^3J_{NC\gamma}$ from K, one can either assume that $^3J_{NC\beta} = {}^2J_{NC\beta} = 0$, or $^3J_{NC\beta} = 0$ and $^2J_{NC\beta} = 0.7$ Hz. For large values of $^3J_{NC\gamma}$, both approaches yield similar results (Table 1). For Ile and Val, it is not possible to distinguish from the difference spectrum alone whether the difference signal originates primarily from $^3J_{NC\gamma 1}$ or $^3J_{NC\gamma 2}$. However, for cases such as Ile[3] or Val[17], where the intensity in the difference spectrum is weak, the χ_1 rotamer assignments are straightforward (+60° and −60°, respectively).

Assuming $^3J_{NC\gamma}T \ll 1/2\pi$, the intensity of the difference spectrum is optimized by setting $T = T_{2N}$, where T_{2N} is the in-phase ^{15}N transverse relaxation time. Therefore, the duration of the ^{15}N constant-time evolution period, $2T - 2\Delta$ (where $\Delta = (2\, {}^1J_{NH})^{-1}$), is unusually long, resulting in highly resolved ^{1}H-^{15}N shift correlation spectra.

The equations presented above assume that the spin state of the aliphatic carbons remains unchanged during the lengthy ^{15}N de- and rephasing periods. However, for the relatively rapidly tumbling ubiquitin protein, ^{13}C T_1 values at 151 MHz are expected to fall in the 0.25–1 s range. Correcting for this finite ^{13}C T_1 is straightforward (Vuister and Bax, 1993; Kuboniwa et al., 1994) and increases J_{NC} by ~16% for $T_1 = 0.25$ s and ~4% for $T_1 = 1$ s, assuming $2T + 4\delta = 200$ ms (Fig. 1) or $2T = 200$ ms (Fig. 2). As the ^{13}C T_1 values for the backbone $^{13}C^\alpha$ atoms in ubiquitin exhibit extensive variations (Wand et al., 1996) and no T_1 values for non-methyl side-chain carbons in

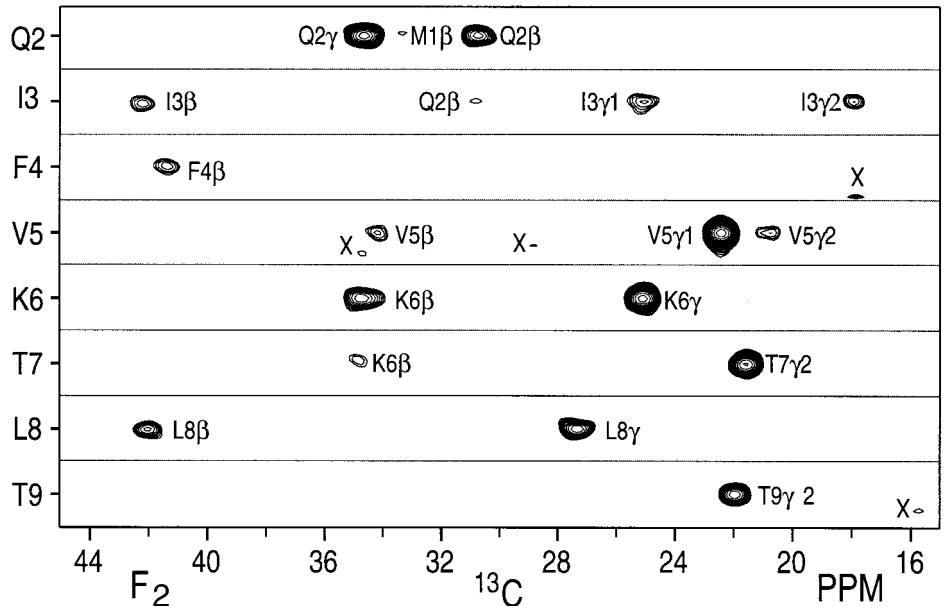

Fig. 3. (F1,F3) strips from the 3D HNCG spectrum of ubiquitin, taken at the $^{1}H^{N}$ (F3) and ^{15}N (F1) frequencies of Gln^{2}-Thr^{9}. Correlations from residues with $^{1}H^{N}$ and ^{15}N shifts in the vicinity of the selected amide strip are marked '×'. The total matrix size was 40*×80*×768*, with a total data acquisition time of 44 h. The 2D reference spectrum (not shown) was recorded as a 128*×768* spectrum.

ubiquitin have been reported, no correction is made. Values reported in this study therefore underestimate the true $^{3}J_{NC\gamma}$ couplings by 5–15 %.

Experiments were applied to samples of 1.5 mM U-$^{13}C/^{15}N$ ubiquitin at pH 4.3 and 30 °C, and 1.5 mM of a complex between U-$^{13}C/^{15}N$ calmodulin and a 26-residue unlabeled peptide fragment of skeletal muscle myosin light chain kinase at pH 6.8, 100 mM KCl, 35 °C. All experiments were carried out on a Bruker DMX-600 spectrometer, equipped with a three-axis pulsed-field gradient, triple-resonance probehead.

A 3D HNCG spectrum of ubiquitin was recorded with the pulse scheme of Fig. 1, using a 40*×80*×756* data matrix, with acquisition times of 24 ms (t_1, ^{15}N), 8 ms (t_2, ^{13}C) and 80 ms (t_3, $^{1}H^{N}$), and a total acquisition time of 44 h. A 2D reference spectrum (128*×756*) was also recorded, using the alternate receiver phase cycling scheme described in the legend to Fig. 1. Figure 3 shows strips taken from the 3D HNCG spectrum at the positions of the amides of Gln^{2}-Thr^{9}. Clearly, correlations to the C^{β}_{i-1} resonance are invariably very weak, corresponding to $^{3}J_{NC\beta}$ couplings smaller than ~0.3 Hz. Values

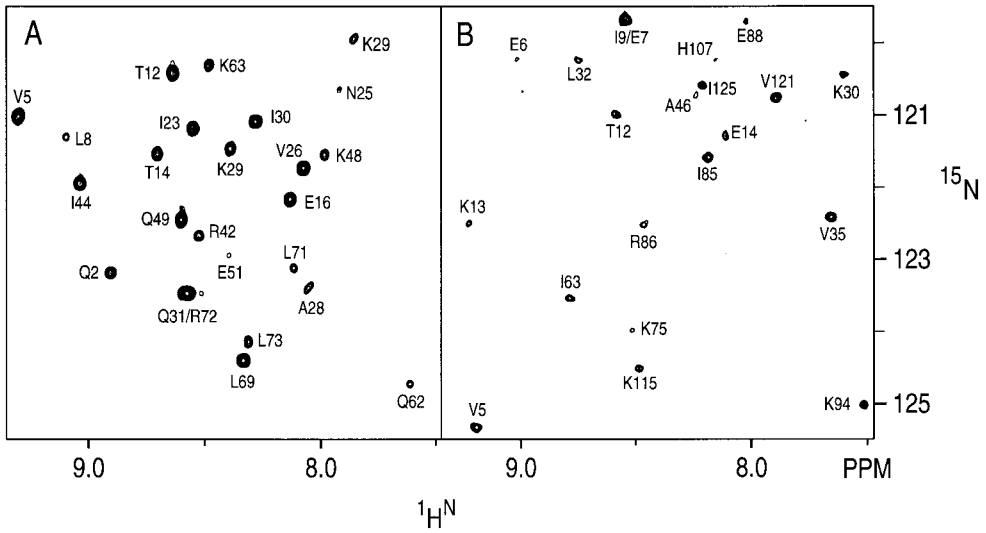

Fig. 4. Small regions of the 2D $^{1}H^{N}$-^{15}N-{$^{13}C^{\gamma}$} difference spectra for (A) ubiquitin, and (B) the calmodulin–peptide complex. The total data acquisition time was 10.5 h for ubiquitin, and 3.1 h for the calmodulin–peptide complex. Only residues with $^{3}J_{NC\gamma}$>~0.7 Hz (A) and >0.9 Hz (B) are visible at the contour levels shown. The ubiquitin spectrum is plotted at a contour level about three times higher than the highest noise, whereas the lowest contours in calmodulin are just above the noise level.

calculated from the intensity ratio of the resonance in the 3D spectrum and the corresponding resonance in the reference spectrum are presented in Table 1.

Figure 4A shows the 2D ^{15}N-{^{13}C} spin-echo difference spectrum of ubiquitin. The spectra with the 180° $^{13}C^{\beta/\gamma}$ pulse in positions a (reference) and b (attenuated) were recorded in an interleaved manner and stored separately. A few weak correlations, e.g. for Ala[28] and Lys[29], have skewed multiplet shapes. These skewed shapes are of the E.COSY type (Griesinger et al., 1985; Eberstadt et al., 1995) and indicate that both ^{15}N and $^{1}H^{N}$ have a common J coupling to a $^{13}C^{\beta}$ or $^{13}C^{\gamma}$. Considering that $^{4}J_{H^{N}C\gamma}$ couplings are vanishingly small, the common coupling must be to the intraresidue $^{13}C^{\beta}$, and the shape of the multiplet serves as a useful indicator that the difference peak has a contribution from $^{2}J_{NC\beta}$. Use of Eq. 5, together with quantitative measurement of the ratio of the $^{1}H^{N}$-^{15}N intensities in the reference and attenuated spectra, permits calculation of $^{3}J_{NC\gamma}$. The results are presented in Table 1. Comparison of the ^{3}J values measured from the 2D spectra with those of the 3D spectrum shows excellent agreement, particularly when the $^{2}J_{NC\beta} = 0.7$ Hz assumption is used (rmsd = 0.11 Hz for all residues with 3D $^{3}J_{NC\gamma} \geq 1$ Hz). Results for $^{3}J_{NC\gamma}$ couplings to methyl groups (2D, assuming $^{2}J_{NC\beta} = 0.7$ Hz; $^{3}J_{NC\gamma'} = 0.4$ Hz for Val and Ile) show good agreement (rmsd = 0.15 Hz) with values that were measured with the ^{13}C-{^{15}N} 2D spin-echo difference method (Vuister et al., 1993). This latter difference decreases to 0.07 Hz if the values from the new measurement are scaled by a factor 1.10, in order to account for the above mentioned effect of the finite ^{13}C T_1 values. As the values from the ^{13}C-{^{15}N} 2D spin-echo difference method also underestimate $^{3}J_{NC\gamma}$, but by a considerably smaller amount (due to shorter de- and rephasing delays and relatively long ^{15}N T_1), the true scaling factor is presumably slightly larger than 1.10.

Figure 4B shows the 2D ^{15}N-{^{13}C} spin-echo difference 2D spectrum recorded for the 20 kDa calmodulin–peptide complex (3 h measuring time). It clearly allows identification of residues with large $^{3}J_{NC\gamma}$ couplings, and quantitative measurement of these ratios shows that only for 16 residues $^{3}J_{NC\gamma} \geq 1.6$ Hz (see Supplementary Material). The $^{3}J_{NC\gamma}$ values complement $^{3}J_{C'C\gamma}$ couplings previously measured for this complex (Hu and Bax, 1997), and together they determine the χ_1 angle for the majority of residues containing aliphatic C^{γ} nuclei.

In summary, we have demonstrated that measurement of $^{3}J_{NC\gamma}$ in isotopically enriched proteins is readily possible for all residues with aliphatic $^{13}C^{\gamma}$ nuclei. In contrast to the ^{13}C-{^{15}N} CT-HSQC difference experiment (Vuister et al., 1993), however, the 2D version of the HNCG experiment described here does not allow $^{3}J_{NC\gamma 1}$ and $^{3}J_{NC\gamma 2}$ in Val and Ile to be measured separately. The measurements are reasonably sensitive and yield excellent results in an overnight experiment on protein samples of ≥1 mM with a rotational correlation time ≤8 ns. For slower tumbling proteins with faster ^{15}N transverse relaxation, or for more dilute samples, acceptable results can be obtained provided that longer measuring times are used.

Acknowledgements

We thank F. Delaglio and D. Garrett for the software used during data analysis, and Stephan Grzesiek for discussions and useful suggestions. This work was supported by the AIDS Targeted Anti-Viral Program of the Office of the Director of the National Institutes of Health. J.-S.H. is supported by a postdoctoral fellowship from the Cancer Research Institute, New York, NY, U.S.A.

References

Archer, S.J., Ikura, M., Torchia, D.A. and Bax, A. (1991) *J. Magn. Reson.*, **95**, 636–641.

Bax, A., Mehlkopf, A.F. and Smidt, J. (1979) *J. Magn. Reson.*, **35**, 167–169.

Bax, A., Ikura, M., Kay, L.E., Torchia, D.A. and Tschudin, R. (1990) *J. Magn. Reson.*, **86**, 304–318.

Clore, G.M., Bax, A. and Gronenborn, A.M. (1991) *J. Biomol. NMR*, **1**, 13–22.

Eberstadt, M., Gemmecker, G., Mierke, D.F. and Kessler, H. (1995) *Angew. Chem., Int. Ed. Engl.*, **34**, 1671–1695.

Emsley, L. and Bodenhausen, G. (1990) *Chem. Phys. Lett.*, **165**, 469–476.

Griesinger, C., Sørensen, O.W. and Ernst, R.R. (1985) *J. Am. Chem. Soc.*, **107**, 6394–6396.

Grzesiek, S. and Bax, A. (1992) *J. Magn. Reson.*, **96**, 432–440.

Grzesiek, S., Ikura, M., Clore, G.M., Gronenborn, A.M. and Bax, A. (1992) *J. Magn. Reson.*, **96**, 215–221.

Güntert, P., Braun, W., Billeter, M. and Wüthrich, K. (1989) *J. Am. Chem. Soc.*, **111**, 3997–4004.

Hu, J.-S. and Bax, A. (1997) *J. Am. Chem. Soc.*, in press.

Hu, J.-S., Grzesiek, S. and Bax, A. (1997) *J. Am. Chem. Soc.*, **119**, 1803–1804.

Kay, L.E., Keifer, P. and Saarinen, T. (1992) *J. Am. Chem. Soc.*, **114**, 10663–10665.

Kraulis, P.J., Clore, G.M., Nilges, M., Jones, T.A., Pettersson, G., Knowles, J. and Gronenborn, A.M. (1989) *Biochemistry*, **28**, 7241–7257.

Kuboniwa, H., Grzesiek, S., Delaglio, F. and Bax, A. (1994) *J. Biomol. NMR*, **4**, 871–878.

Palmer, A.G., Cavanagh, J., Wright, P.E. and Rance, M. (1991) *J. Magn. Reson.*, **93**, 151–170.

Peng, J.W. and Wagner, G. (1992) *J. Magn. Reson.*, **98**, 308–332.

Silver, M.S., Joseph, R.I. and Hoult, D.I. (1984) *J. Magn. Reson.*, **59**, 347–351.

Sørensen, O.W. (1990) *J. Magn. Reson.*, **96**, 433–438.

Vuister, G.W. and Bax, A. (1993) *J. Am. Chem. Soc.*, **115**, 7772–7777.

Vuister, G.W., Wang, A.C. and Bax, A. (1993) *J. Am. Chem. Soc.*, **115**, 5334–5335.

Wagner, G., Braun, W., Havel, T.F., Schaumann, T., Gō, N. and Wüthrich, K. (1987) *J. Mol. Biol.*, **196**, 611–639.

Wand, A.J., Urbauer, J.L., McEvoy, R.P. and Bieber, R.J. (1996) *Biochemistry*, **35**, 6116–6125.

Wang, A.C. and Bax, A. (1995) *J. Am. Chem. Soc.*, **117**, 1810–1813.